

Chapter 3

Experimental arrangement

Total attenuation coefficient of a material is a measure of the interaction of gamma rays that took place in the given material. After each single event of interaction the incident photon continues to exist with or without energy degradation, except in the case of photoeffect, where the incident photon is completely absorbed in a single event. Following photo absorption, photoelectrons are emitted creating an electron vacancy in the atom (mostly in the *K-or* L-shell). The ensuing rearrangement of the remaining electrons is accompanied by the emission of one or more X-ray photons (characteristic X-rays) or auger electrons or both. The photoelectrons, pair production electrons & positrons and auger electrons so produced, may interact with the Coulomb field of atomic nucleus, resulting inelastic collisions, which in turn produces Bremsstrahlung radiation. All these secondary photons produced inside the attenuator due to single events of interactions, may be scattered and rescattered, inside a sample of sufficient thickness, at such angles, that they finally reach the detector. An accurate analysis and evaluation of the secondary radiations is exceedingly tedious. It is very difficult to separate low angle scattered photons from the uninteracted transmitted beam. This fact makes the total attenuation coefficient measurement a highly complicated and difficult one. Unless the experimenter takes extreme

care in designing the geometry, taking in to account the factors like the energy of the primary photons, the source strength, nature of the absorber material, the detecting system to be used etc. the possibility of obtaining reliable results is very little. Experimental configurations and problems associated with the measurement of X-ray attenuation coefficients has been discussed by Creagh and Hubbell (1987, 1990) and Creagh (1992).

Depending on the design, geometrical setup may be divided in to two categories, good geometry and bad geometry.

3.1 Narrow Beam Geometry

In a narrow beam (good) geometry febts geometrical setup the primary beam is collimated by shields or collimators with appropriate co-axial circular apertures. The collimated beam of gamma rays travels along the line joining centres of the point source of gamma rays and the detector. The attenuator (or absorber) in the form of a cylinder is interposed with its axis along the line joining the source and the detector. We shall assume that no scattered photon reaches the detector, which is possible only if the diameter of the cylinder is much less than the mean free path of the photon. Of-course, in such a case the probability for a scattered photon to be deflected out of the cylinder through the lateral surface is very large, and which in turn considerably reduces their possibility to reach the detector. Such a geometry is said to be a good geometry. In practice in a good geometry setup the scattered photons reaching the detector shall be either negligible or quantitatively determined. Here the incident intensity I_o is related with the transmitted intensity I by equation (1.1).

3.2 Bad Geometry

If the diameter of the absorber cylinder is almost equal to or greater than the mean free path of the photons, the scattered photons will have more probability for multiple scattering inside the sample material, and finally to emerge out in appropriate angles to reach the detector. This results in an overestimation of the transmitted intensity and underestimation of the corresponding attenuation cross section. The geometry is now called *broad beam or bad geometry*. Accurate evaluation of broad beam attenuation is exceedingly difficult due to the multiple scattering effects.

3.3 Experimental setup used by different experimenters

In the total attenuation coefficient measurements one should make sure that no scattered Bremsstrahlung, or annihilation photons (secondary radiations) reach the detector. Their arrival at the detecting system will result in an overestimation of the transmitted intensity which corresponds to an underestimation of the cross section. Most of the experimenters in this field have used a narrow beam geometry to attain this objective.

It was Davisson and Evans (1951) who introduced for the first time, a good geometry setup, for the measurement of total attenuation cross sections of gamma rays in elements. Special care has been taken by them in designing the geometry of the experiment to see that the scattered photons reaching the detector is negligible. They have used a well collimated beam of apex angle about 1 degree, with three lead collimators at appropriate distances between the gamma ray source and the detector. Lead shielding has been provided, both for the source and the detector, so as to prevent the possibility of gamma rays getting scattered from the surrounding objects

and finally reach the detector. With this geometry they made a detailed investigation of gamma ray interaction of Al, Cu, Sn, Ta and Pb attenuators with various intermediate energy photons. The results obtained in the energy range 500 to 2800 keV showed good agreement with the theoretical values and the values obtained by other experimenters. Appreciable deviations were reported in the results, for photons from Zn^{65} and Co^{60} .

The secondary radiations, which include Compton scattered, coherently scattered and Bremsstrahlung photons, reaching the detector may be minimized by:

1. by reducing the angle of acceptance, for the scattered photons from the attenuator to the detector and
2. by selecting a suitable attenuator thickness, in a narrow beam geometry setup.

Wiedenbeck (1962) has used an effective solid angle of acceptance 3×10^{-7} steradian for scattered radiation, in their investigations where as Perkin and Douglas (1967) used a solid angle 0.01 steradian.

To minimize the multiple scattering effects McCrary et al. (1967) and Conner et al. (1970) have selected a range of value 0.01 to 0.4 for the ratio I/I_0 .

Sinha and Chaudhuri (1973) have chosen such a sample thickness that the FWHM of the photopeak remained the same in the cases with and without the sample.

Gopal and Sanjeevaiah (1973_a & 1973_b) used a condition $\mu t < 1$ in their investigations, along with the counting sequence of Conner et al. (1970), to reduce the multiple scattering effects.

Puttaswamy et al. (1980) have used an extrapolation technique to correct for the multiple scattering effects on the transmitted intensity.

When composite energy gamma ray sources have to be used, where

the difference of successive energies is not so large, the detecting system should have very good resolution. The energy resolution of Geiger counter, proportional counter, ionization counter etc. is very poor. Hence measurements using them yield composite absorption coefficients. NaI(Tl) crystal scintillation detector is having better resolution and is much more efficient than many other detectors. The semiconductor detectors like Ge(Li), Si(Li), High-Purity Germanium etc. are having optimum efficiency and better percentage resolution than the NaI(Tl) scintillation detectors. So they may be employed with more advantage, in dealing with composite energy gamma ray sources.

A High-Purity Germanium detector, having good resolution and optimum efficiency, was used in the current study for the measurement of total attenuation cross sections of most of the amino acids and several sugars for gamma ray photons from ^{133}Ba , ^{60}Co , ^{137}Cs and ^{141}Ce sources. A description of the geometry used in the experiment is given in the following section.

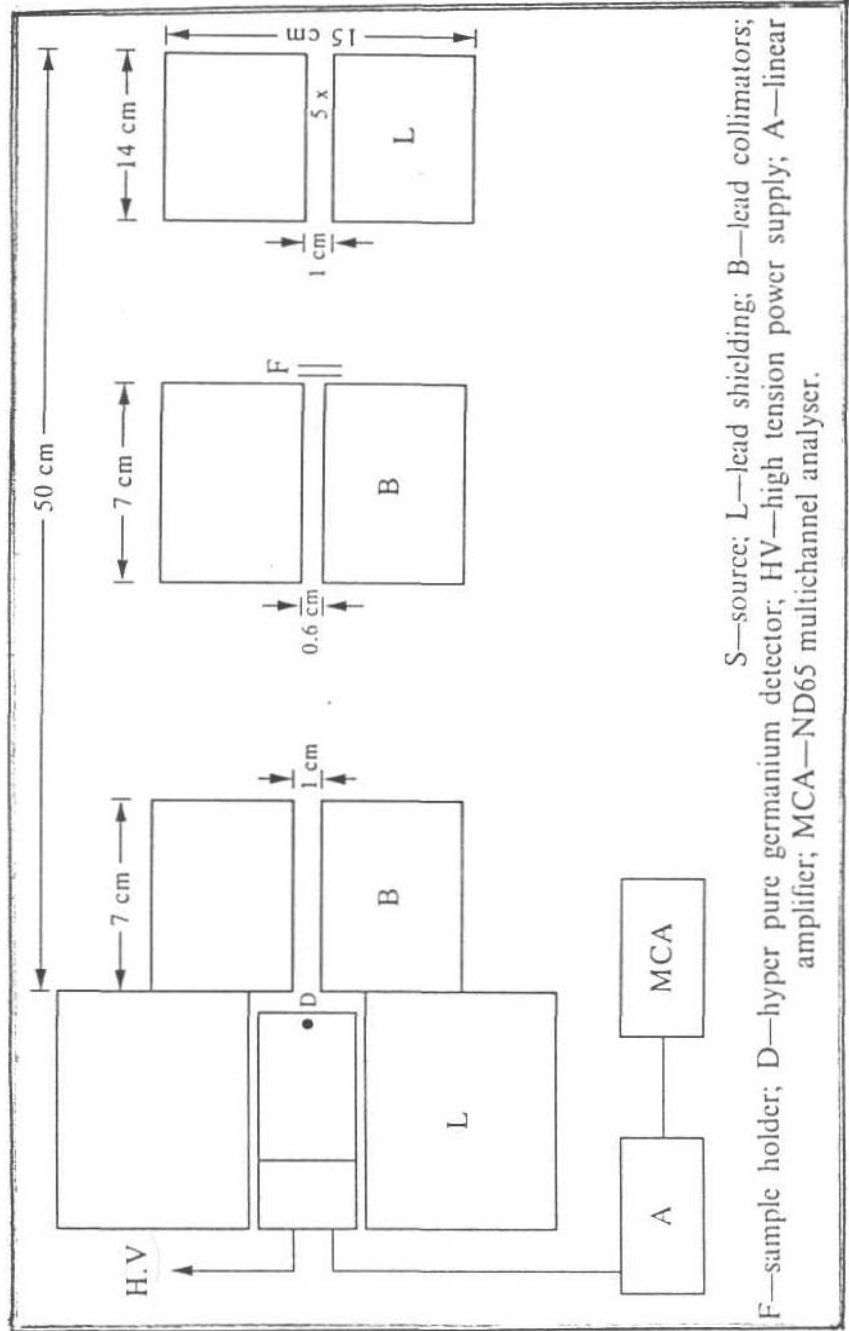
3.4 The Geometry used in the current work

The geometrical arrangement along with the counting and spectrum recording system is shown in figure 3.1.

Design of the geometry assumes great significance due to the fact that the accuracy of results mainly depends on it. For reasons explained in the beginning of this chapter, a good geometry setup was employed in the current experiment. In designing the geometry, care has been taken to prevent the secondary radiations from reaching the detector. The secondary radiations are produced not only inside the absorber but also in the surrounding objects, which are exposed to the incident radiation. To prevent these radiations from entering the detector the geometry may be designed in any of the following methods.



Experimental arrangement along with the counting and spectrum recording system



S—source; L—lead shielding; B—lead collimators; F—sample holder; D—hyper pure germanium detector; HV—high tension power supply; A—linear amplifier; MCA—ND65 multichannel analyser.

Figure 3.1: Experimental arrangement along with the counting and spectrum recording system

In the first method the source-detector and absorber-detector distances are kept large. The angular separation of the scattered radiation increases with distance which in turn reduces the angle of acceptance for the scattered radiation at the detector. So the possibility of secondary radiations entering the detector reduces with large source-detector and absorber-detector distances.

In the second method thick lead shielding is provided to the source and the detector, which will reduce the possibility of scattering of gamma radiation from the near by objects. If a few photons are scattered, they will be stopped by the thick lead shielding surrounding the detector.

Intensity of gamma radiation reaching the detector will be considerably reduced if the source-detector distance is increased above an optimum value. Otherwise one should use more powerful gamma sources. Moreover a large source-detector distance creates several practical difficulties. The second method does not involve these problems and is more effective in shielding the secondary radiations. It needs only reasonable source-detector distance, which avoids the use of strong sources. So the second method is made use of in the current geometry. It has effectively ruled out any possibility for the photons scattered from the nearby objects to reach the detector.

The amount of secondary radiations produced inside the attenuator and reaching the detector may be estimated by considering the geometrical setup and the characteristics of the secondary radiations produced. If the maximum angle of scattering available for the scattered photons from the attenuator to the detector is θ_{max} , the intensity of Compton scattered photons within a solid angle defined by θ_{max} is given by the relation

$$N = \frac{N_o Z}{A} r_o^2 t \theta_{max}^2 \left[1 - \frac{\theta_{max}^2}{12} (9K + 4) \right] \quad (3.1)$$

where N_o is the Avogadro number, Z , A and t are respectively atomic number, atomic weight and thickness of the scatterer and K is the incident

photon energy in units of m_0c^2 . This formula is deduced from the KN formula (Davisson and Evans 1951). The intensity N if subtracted from the transmitted intensity I would give the value of I corrected for the Compton scattering through θ_{max} .

In addition to the Compton scattering, coherent scattering also assumes significance, especially in the low angles of scattering. So the transmitted intensity I has to be corrected for this effect also. The intensity of photons due to coherent scattering within a solid angle defined by θ_{max} can be obtained by integrating numerical data of Debye (1923) and the equations of Franz (1935). Hubbell and Berger (1968) have tabulated values of these small angle scattering cross sections for a few elements.

As explained in section 3.3 the sample thickness was optimized such that $0.1 < \mu t < 0.4$, to reduce the multiple scattering effects. The minimum effects of multiple scattering have been corrected for by an extrapolation technique [Puttaswamy (1980)]. This is explained in detail in chapter 4,

The maximum angle of acceptance θ_{max} , for the scattered photons at the detector was 31 minutes, which has considerably reduced the solid angle. So the number of scattered photons reaching the detector has been minimized (Davisson and Evans 1951). It also makes the count rate less sensitive to the absorber position (Howland and Kreger 1954).

3.5 Samples

The samples of amino acid and sugar compounds used in the current work were manufactured by M/S Fluka A.G.Switzerland. All the samples were of analar grade. The typical impurities as specified by the manufacturer are: chlorine $< 0.01\%$, iron, copper, zinc, cadmium, and lead each $< 0.0001\%$. The samples were taken in their powder form, because in the transmission experiments samples in their solid form are more convenient and preferable

than that in their liquid or gaseous forms. Each compound under investigation was confined in cylindrical plastic containers of inner diameter about 1.4 cm. with suitable length to have an optimal thickness (section 3.3 and 3.4.). The inner diameter of each container was separately determined by using a travelling microscope. The measurement was repeated several times for each container separately. The average of these values was taken as the diameter of the container. The mass of each sample was determined, correct to fraction of a milli gram, using a digital balance. The weighing was repeated several times to get concordant values of the mass. Mean of these concordant values was taken to be the mass of the sample.

Using the average value of the inner diameter of the plastic container and mass of the sample, the mass per unit area was determined for each sample. The uncertainty in the value of mass per unit area in each case was less than 0.05%

Non-uniformity of the sample material was checked by exposing different parts of the sample to the incident photon beam. Any discrepancy in the intensity was found to be within the counting statistics. This fact confirmed that the error due to non-uniformity of the sample was negligible.

The error due to sample impurity could be a significant factor only when large percentages of high Z impurities are present in the sample. However in all the samples used in the experiment, the content of high Z impurities was less than 0.005%. Hence the sample impurity correction was negligibly small.

The sources of errors are discussed in more detail in chapter 4.

A list of amino acid and sugar compounds used in the investigation are given respectively in Tables 3.2 and 3.1 along with their respective formulae and molecular weights.

Table 3.1: List of the Sugars
along with their chemical formula and molecular weight.

Sl.No.	Sugar	Chemical symbol	Molecular weight
1	Arabinose	$C_5 H_{10} O_5$	150.14
2	Ribose	$C_5 H_{10} O_5$	150.14
3	Glucose	$C_6 H_{12} O_6$	180.14
4	Galactose	$C_6 H_{12} O_6$	180.14
5	Mannose	$C_6 H_{12} O_6$	180.14
6	Fructose	$C_6 H_{12} O_6$	180.14
7	Rhamnose	$C_6 H_{12} O_5, H_2O$	182.2
8	Maltose	$C_{12} H_{22} O_{11}$	342.3
9	Melibiose	$C_{12} H_{22} O_{11}$	342.3
10	Melezitose	$C_{18} H_{32} O_{16} H_2O$	522.5
11	Raffinose	$C_{18} H_{32} O_{16}, 5H_2O$	594.5

Table 3.2: List of the Amino acids
 Along with their chemical symbols and molecular weights.

Sl.No.	Amino acid	Chemical symbol	Molecular weight
1	Glycine	$C_2 H_5 NO_2$	75.1
2	Alanine	$C_3 H_7 NO_2$	89.1
3	Serine	$C_3 H_7 NO_3$	105.1
4	Valine	$C_5 H_{11} NO_2$	117.1
5	Threonine	$C_4 H_9 NO_3$	119.1
6	Leucine	$C_6 H_{13} NO_2$	131.2
7	Isoleucine	$C_6 H_{13} NO_2$	131.2
8	Aspartic Acid	$C_4 H_7 NO_4$	133.1
9	Lysine	$C_6 H_{14} N_2 O_2$	146.2
10	Glutamic Acid	$C_5 H_9 NO_4$	147.1
11	Histidine	$C_6 H_9 N_3 O_2$	155.2
12	Phenyl Alanine	$C_9 H_{11} NO_2$	165.2
13	Argioine	$C_6 H_{14} N_4 O_2$	174.2
14	Tyrosine	$C_9 H_{11} NO_3$	181.2
15	Tryptopline	$C_{11} H_{12} N_2 O_3$	204.2
16	Cystine	$C_6 H_{12} N_2 O_4 S_2$	240.2

3.6 Radioactive sources

The radioactive sources of gamma rays used in this investigation are given in Table 3.3 along with their half lives, strength and energy. These sources either in the form of radiographic capsules or (plastic) discs were obtained from the Bhabha Atomic Research Center, Bombay, India.

3.7 The detection system - Gamma ray spectrometer

The gamma ray spectrometer includes, the photon detector, bias supply units, pre amplifier spectroscopic amplifier, analog to digital converter (ADC) and a multichannel analyser (MCA). A high pure Germanium detector with high resolution and optimum efficiency was employed in the transmission experiment, which has effectively resolved the multienergy photons from the composite energy photon sources used.

3.8 High-Purity Germanium detector

The EG & G Ortec High-Purity Germanium Gamma-X coaxial detector system has a nominal total active area of 110 cm². It has a central Beryllium window of 0.5 mm thickness at a distance of 6 mm from the detector surface, which enables even the low energy photons to penetrate in to the active volume of the detector. The detector has a resolution of 2.1 keV at 1332.5 keV and 23% efficiency. The preamplifier and the high-voltage filter are connected electrically to the detector through vacuum seals. The crystal is designed to keep the detector at 77 K (liquid nitrogen temperature) and in a sealed vacuum for fairly long time. The first FET of the preamplifier is mounted inside the end cap and cooled to achieve very good resolution.

Table 3.3: List of radioactive sources
used in the investigation.

Sl. No.	Radioactive sources	Half life	Energy
1	^{133}Ba	7.5 years	30.8 keV 35 keV 81 keV 276.4 keV 302.9 keV 356 keV 383.9 keV
2	^{141}Ce	32.5 days	145 keV
3	^{137}Cs	30 years	661.6 keV
4	^{60}Co	5.24 years	1173 keV 1332.5 keV

Unlike Ge(Li) detectors, HPGe detectors disconnected from all external circuits may be warmed up to room temperature and stored for any desired period and then cooled again. So it is enough to cool it and keep at liquid nitrogen temperature only during the actual course of the experiment. However special care has to be taken during each first cooling to see that the high voltage is applied only after a minimum of six hours cooling time. It will prevent any possibility of damage of the detector due to electrical sparking.

The operating voltage of the detector was 2500 volts and was operated at the liquid nitrogen temperature.

3.9 Spectroscopy with gamma-X detectors

The semiconductor detector material absorbs energy from the incident gamma ray photon and generates a current pulse whose integral in time domain has an amplitude that is proportional to the absorbed energy. This current pulse is amplified by the preamplifier, attached to the detector assembly. The preamplifier out put is fed to an ADC and finally to a multi-channel analyser (MCA). The MCA records spectrum of the transmitted gamma rays in its memory. Brief discussion of the detector bias supply, spectroscopy amplifier and the MCA used are given in the following sections.

3.10 Ortec 459 5 kV detector bias supply

The *Ortec* 459 0-5 kV detector bias supply unit provides two separate out puts simultaneously. One out put is in the range 0-5 kV for high voltage requirements and the other in the range 0-500 V for lower voltage detectors. The two out put voltages are adjustable by a five turn direct reading control through potentiometer located on the front panel. The required polarity

can be selected by the orientation of a plug in printed circuit attached to the main board in either of the two positions. The selected polarity would be indicated by an indicator lamp. A front panel meter also indicates the selected polarity and the voltage available through the 5 kV out put. The 500 V out put provides 10% of the level through the 5 kV out put. The input to this power supply unit was stabilized using a *Krykard* voltage stabilizer, having an in-built line filter.

3.11 Ortec 571 Spectroscopy amplifier

The *Ortec 571* spectroscopy amplifier is a single width NIM module with a versatile combination of switch selectable pulse-shaping and out put characteristics. It features extremely low noise, ($< 8\mu$ V for 2 μ s shaping and gain 100), wide gain range (1 to 1500 continuously) and excellent overload response for universal application in high-resolution spectroscopy. It accepts input pulses of either polarity of rise-times < 650 ns and fall times $> 40\mu$ s.

This amplifier has an input impedance of 1000 ohms and six integrate and differentiate time constants for optimum shaping to achieve specified resolution and count rate. The first differentiation net work has variable pole-zero cancellation that can be adjusted to match preamplifiers with decay times $> 40\mu$ s. The pole-zero cancellation drastically reduces the undershoot after the first differentiator and greatly improves overload and count-rate characteristics. In addition, the amplifier contains an active filter shaping network that optimizes the signal to noise ratio and minimizes the overall resolving time. This provides both unipolar and bipolar outputs simultaneously. The power supply required for the detector preamplifier is supplied by this amplifier unit.

3.12 Multichannel Analyzer

The multichannel analyzer (MCA) performs the essential function of collecting the data, providing a visual display and output, either in the form of final results or data for later analysis. MCA may be operated in the Pulse Height Analysis (PHA) mode as well as in the Multi Channel Scaling (MCS) mode. PHA is the traditional operating mode of MCAs. PHA mode was used in this work. It is used for accumulation of a spectrum of the frequency distribution of the heights from a sequence of random input pulses produced from photon detectors.

Two multichannel analyzers have been used in this work. An ND-65 MCA was used for acquisition of data, in the initial stages. A PC-based MCA was used for the acquisition of data as well as its analysis, in the latter stages of the work. A description of these two MCAs is given in sections 3.11.1 and 3.12.2.

3.12.1 ND-65 MCA

The ND-65 is a firmware controlled, microcomputer-based, multichannel analyzer system with the capability of being operated both as a stand-alone analyzer and a remote computer terminal. It combines the operational convenience of a hardware MCA with the computational power of a LSI-11/2 microcomputer to produce a powerful yet easy-to-use multichannel data acquisition and analysis system.

The ND-65 MCA provides complete data acquisition, storage, display, manipulation and input/output capability and flexibility. It supports PHA, MCS or list mode acquisition. Basic data storage memory is 4 K, 24-bit data channels expandable up to 8 K. A comprehensive alpha-numeric display of system parameters simultaneous with linear or logarithmic spectral data display keeps the user constantly informed of system status. Optical

firmware drivers and interfacing are available for a variety of peripheral options including terminal printers, line printer and video copier. The keyboard, containing a total of 56 keys is the data entry and control center of the ND-65 system.

There is a built-in Analog to Digital Converter (ADC) in the ND-65 MCA. It is designed for high resolution processing of amplitude modulated signals of the type encountered with when measuring fast, random phenomena. The ADC contains a delay-line amplifier, passive baseline restorer, pulse amplitude to time converter, 13-bit address scalar and control circuitry. The data acquisition efficiency of this MCA is enhanced by a 80 MHz digital rate. The digitizing oscillator is crystal controlled to ensure frequency stability. Above all, every critical circuitry is temperature compensated to ensure drift-free operation. Conversion gain is selectable in binary increments 256 to 8192 channels full scale. Analog zero is adjustable between $\pm 5\%$ of full scale via a front panel, multiturn potentiometer.

Both upper and lower level discriminators are variable from 0 to 110% of full scale via front panel, multiturn, locking potentiometers. Upon acceptance of an event, the lower level discriminator is locked out of operation until completion of an ADC cycle. If, at the time it is re-enabled, the input level is higher than the discriminator threshold (indicating an event at the linear gate), the ADC does not accept the event for analysis. The operation of the upper level discriminator provides a fast dump feature which rapidly discharges from the data handling circuitry. These features provide a significant reduction in system dead time. Inputs to the ADC can be supplied directly from an external preamplifier/amplifier combination. For PHA acquisition, ADC digital offset may be selected from 0 to 8191 channels.

The desired acquisition mode, preset time (sweeps), digital offset, and dwell time are entered via simple commands at the ASCII key board and

displayed as acquisition status parameters.

During acquisition, the system automatically computes and displays the elapsed real and live times, and the total counts, net area (total counts minus back ground counts), back ground counts and counts per second in the channel between, and including the left and right marker channels. Data can be selectively acquired in separate memory groups ranging in size from 256 to 8192 channels to permit acquisition and storage of multiple spectra for comparison, stripping or additional processing functions. The spectrum stored in any memory group can be multiplied by a constant and added to, or subtracted from the spectrum in any other group.

3.12.2 Nucleonix PC MCA 1002

Nucleonix MCA, type: MC 1002 is a personal computer (PC) based system. It has a hard-wired analyzer that accomplishes the data accumulation, storage, display and output function associated with the analysis of the spectrum and reduction capabilities within the system. The PC is an integral part of the MCA operation. The PC, under the control of special-purpose software, is responsible for functions such as controlling data acquisition, generation of display information, and preset conditions etc. All these functions would be performed by circuitry in a hard-wired MCA.

The MCA nuclear data acquisition system consists of

1. Nuclear Analog to Digital Converter (ADC) and
2. Multichannel buffer card.

3.12.3 Analog to digital converter

ADC in the current unit is a Wilkinson-type 3-width NIM style unit. The ADC accepts analog 0-10 volts amplitude unipolar or positive-leading

bipolar pulses from the linear/spectroscopic pulse amplifier outputs, and are digitized into a binary address which is proportional to the peak amplitude of the analog input pulse. The channel number is the memory address. From the output of ADC the memory address is transferred to the multi-channel buffer card, which is suitably interfaced to a personal computer. Corresponding to each digitized pulse a count is added to the appropriate memory location, depending on the channel number. Thus, a spectrum of number of pulses versus voltage pulse height is obtained. The range of channels available with this multichannel analyzer is a minimum of 256 to a maximum of 4096. Therefore ADC resolutions are available from 256 to 4096 channels.

In addition to the basic function of converting the analog input to a binary address, the ADC performs several logic functions to preclude storage of erroneous data due to address overflow, under flow, partial pulses etc.

Multichannel buffer card

Multichannel buffer card functions as an acquisition interface to the computer and contains a memory sub-system within it. At the command of the PC, buffer transfers the data, acquired through the ADC, to the personal computer.

Personal computer

An IBM compatible personal computer is employed as the central unit of the Nucleonix MCA. The personal computer executes the functions of control, data storage and processing with the Nucleonix MCA software. The computer interacts with multichannel buffer for transferring raw acquired data.

The PC Keyboard acts as the medium through which one can in-

interact with the MCA system. The operations of the MCA are completely controlled by MCA System Commands. The user should enter the System Commands through the Keyboard, which then will be executed by the PC. Monitor connected with the PC acts as the MCA display medium for live acquisition, spectrum and data processing.

A Dot Matrix Printer connected to the PC serves as the output medium for getting hard copy print out of the spectral data, data processing results and the spectrum display.

The facilities available for data processing are:

1. The region of interest of the spectrum may be selected with the help of two markers (upper and lower markers).
2. Provisions for Spectrum smoothing, Energy calibration, Computation of energy and Spectrum normalization.
3. Facility to read gross/net area, FWHM, and Peakchannel.

Spectrum smoothing: enables smoothing of the entire spectrum or a region of interest selected by the two markers, to eliminate background undulations. A minimum of 5 points are to be included in the region of interest for smoothening.

Energy calibration: a least squares fit to two or more energy values and channel numbers calibrates the ADC range in energy level.

Computation of energy: enables to read energy for any desired channel number.

Spectrum normalization: the data corresponding to each channel in the spectrum may be multiplied, increased or decreased by a factor, for comparison with other spectra.

Area: computes gross and net area between the lower and upper markers (region of interest).

FWHM : presents the total number of channels within the region of interest, bracketed by the two markers, whose data value is $> 50\%$ of maximum data value in any channel in the selected region.

Peak channel: displays the peak channel within the region of interest, as a number. If the region of interest contains more than one peak, the first peak from the lower marker is presented.

3.13 Calibration of the gamma ray spectrometer

For satisfactory performance of the gamma ray spectrometer it should have very good resolution, linearity and stable operating conditions.

The percentage resolution of the HPGe detector is defined as the ratio of the full width at half maximum (FWHM) of the photopeak times 100 to the photopeak channel number. The resolution is also defined as the product of FWHM in channels and the energy slope calibration in keV/channel. In the current study detector resolution was calculated using a ^{60}Co source, as a function of the operating high tension voltage. The value obtained is about 2.1 keV at 1332.5 keV photopeak for 2500 kV operating voltage.

3.13.1 linearity check

The linearity between the photopeak channel number (pulse height at the photopeak) and photon energy was studied using the sources listed in Table 3.4. Two calibration curves, one up to 500 keV and the other up to 2 MeV, were drawn. They are shown in Figure 3.2. The straight line curve obtained indicates an excellent linearity over the energy range of interest.

To provide very stable operating conditions, the input power supply was regulated and to maintain the room temperature and humidity at a

lower constant level the experiment was performed in an air-conditioned laboratory. Above all, before starting the experiment, a warming-up time of 24 hours was given for the spectrometer. These steps have effectively controlled any drift in operating conditions of the spectrometer like voltages and amplifier gain. However the stability was checked periodically. The periodic checking showed a very good linearity within 1%.

Table 3.4: List of calibration sources
used in the linearity experiments.

Sl. No.	Radioactive sources	Half life	Energy
1	^{133}Ba	7.5 years	30.8 keV 383.9 keV
2	^{141}Ce	32.5 days	145 keV
3	^{203}Hg	47 days	68.89 keV 279.2 keV
4	^{22}Na	2.6 years	511 keV
5	^{137}Cs	30 years	661.6 keV
6	^{60}Co	5.24 years	1173 keV 1332.5 keV

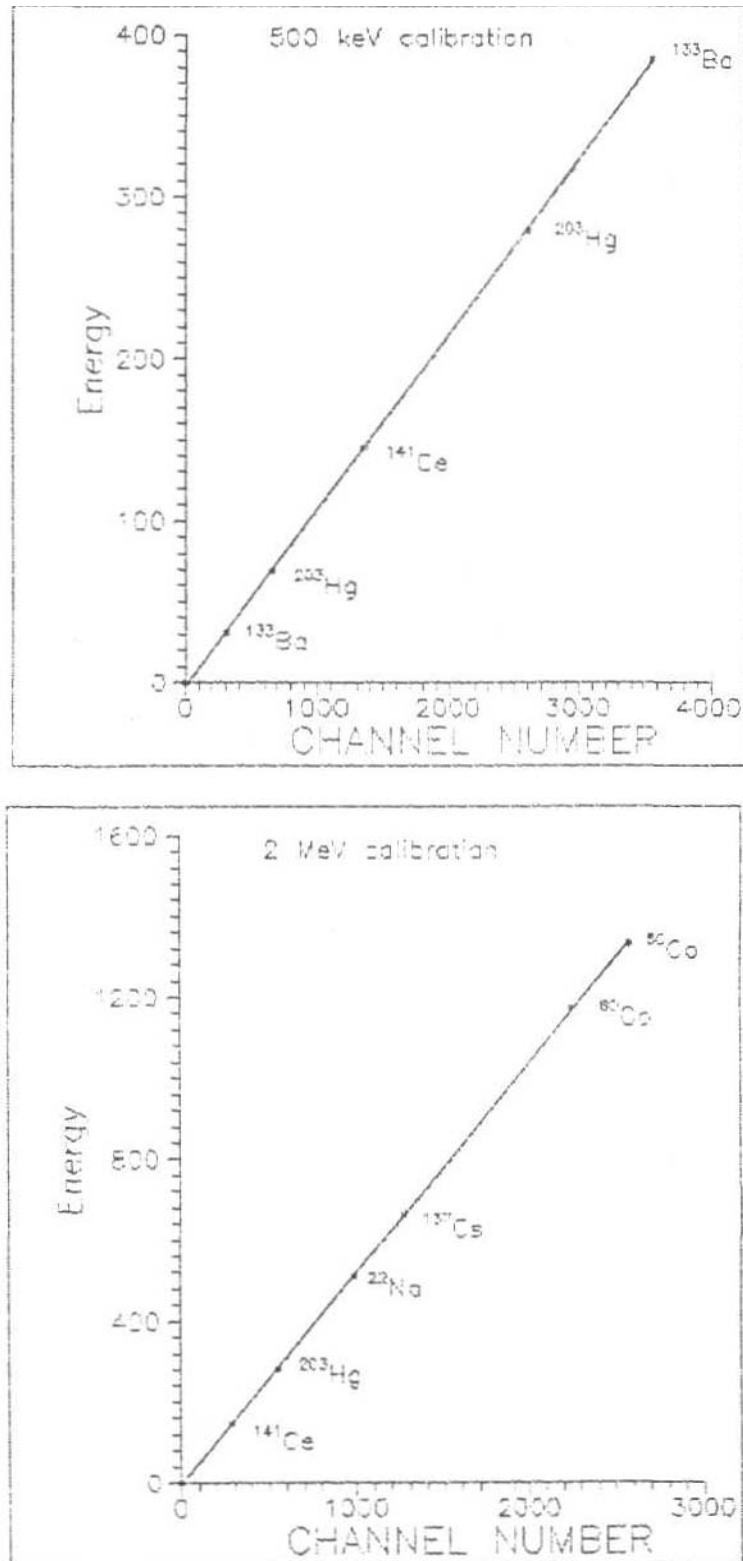


Figure 3.2: Calibration curves, plotted with peak channel number versus energy.